INTERACTIONS BETWEEN MAGMA AND WASTE CONTAINERS

Prepared for

U.S. Nuclear Regulatory Commission
Contract NRC–02–07–006

Prepared by

Ken Chiang
Center for Nuclear Waste Regulatory Analyses
San Antonio, Texas

September 2011

ABSTRACT

Alloy 22 (Ni–22Cr–13Mo–4Fe–3W) was considered as the nuclear waste container material for the proposed Yucca Mountain repository. Under an igneous disruptive event, the waste container material may be deformed or damaged by molten magma at elevated temperatures. In the igneous activity scenario, significant pressure differences between ascending magma and open drifts cause magma to flow into the drifts and fill them upon intersection; thus, waste containers could be engulfed in magma. The ability of a waste container to withstand the combined thermal, chemical, and mechanical effects of magma exposure is uncertain. The Center for Nuclear Waste Regulatory Analyses conducted an independent assessment of magma–Alloy 22 interaction. A methodology was developed to examine magma–Alloy 22 interaction by remelting Lathrop Wells basalt from Nevada in crucibles of Alloy 22. A test methodology was also developed to evaluate the dry-air oxidation behavior of the waste container materials that were not in direct contact with the molten magma. The interaction of molten Lathrop Wells magma with Alloy 22 resulted in two types of corrosion morphology. Accelerated corrosion was observed at the interface where solid metal, liquid magma, and gaseous oxygen coexisted. At locations with low oxygen partial pressures, the Alloy 22 formed continuous chromia scale that results in a low oxidation rate similar to that of dry-air oxidation.

CONTENTS

Section Page

ABSTRACT ii
FIGURES iv
TABLE v
ACKNOWLEDGMENTS vi

1 INTRODUCTION 1-1

2 DRY-AIR OXIDATION 2-1

3 MAGMA–ALLOY 22 INTERACTION 3-1
    3.1 Analyses of Magma Samples from Lathrop Wells Volcano 3-1
    3.2 Alloy 22−Lathrop Wells Magma Interaction Experiments 3-3

4 ANALYSIS OF RESULTS AND DISCUSSION 4-1

5 SUMMARY AND CONCLUSIONS 5-1

6 REFERENCES 6-1

FIGURES

Figure Page

2-1 Schematic Diagram of a Thermogravimetric Apparatus With Automatic Recording Microbalance 2-2
2-2 Photograph of a TherMax700 Automatic Recording Microbalance at Southwest Research Institute® 2-3
2-3 Dry-Air Oxidation Kinetics of Alloy 22 at 850 and 1,100 °C [1,562 and 2,012 °F] Plotted as Mass Change Versus Square Root of Time 2-4
2-4 Cross Section Through the Scale Produced on Alloy 22 After 120 Hours Oxidation at 850 °C [1,562 °F] 2-5

3-1 (a) Photograph of Magma Basalt Samples Collected From Lathrop Wells Volcano in Nevada and (b) Energy-Dispersive X-Ray Spectra of the Magma Sample 3-2
3-2 Drawing of the Alloy 22 Crucible for Magma–Alloy 22 Interaction Experiments 3-3
3-3 Photograph of Alloy 22 Crucible With LW-4 Basalt 3-5
3-4 Scanning Electron Micrographs Showing Cross Sections of Alloy 22 Crucible After Interaction With LW-4 Samples for 65 Hours in Air 3-6

4-1 Comparison of High-Temperature Corrosion Rate of Alloy 22 in the Presence of Remelted Lathrop Wells Basalt at 1,150 °C [2,102 °F] in Air With Published Data on Ni-Cr Alloys 4-2

TABLE

Table Page

2-1 Chemical Composition (wt%) of Alloy 22 Plate 2-3

ACKNOWLEDGMENTS

This report was prepared to document work performed by the Center for Nuclear Waste Regulatory Analyses (CNWRA®) for the U.S. Nuclear Regulatory Commission (NRC) under Contract No. NRC–02–07–006. The activities reported here were performed on behalf of the NRC Office of Nuclear Material Safety and Safeguards, Division of High-Level Waste Repository Safety. The report is an independent product of CNWRA and does not necessarily reflect the views or regulatory position of NRC.

The author gratefully acknowledges R. Pabalan for his technical review, D. Pickett for his programmatic review, L. Mulverhill for her editorial review, and A. Ramos for his secretarial support. The author would like to thank J. Stamatakos and A. Chowdhury for their assistance and support throughout the study.

QUALITY OF DATA, ANALYSES, AND CODE DEVELOPMENT

DATA: All CNWRA-generated data contained in this report meet quality assurance requirements described in the Geosciences and Engineering Division Quality Assurance Manual. Experimental data have been recorded in CNWRA Scientific Notebook Numbers 617, 790, and 840 (Chiang, 2007, 2006, and 2004). Sources of other data should be consulted for determining the level of quality of those data.

ANALYSES AND CODES: None.

REFERENCES

Chiang, K. “Interaction Between Magma and Waste Package Materials.” Scientific Notebook 840. San Antonio, Texas: CNWRA. pp. 33, 105, and 106. 2007.

_____. “Interaction Between Magma and Waste Package Materials.” Scientific Notebook 790. San Antonio, Texas: CNWRA. pp. 8, 16, 22, and 25. 2006.

_____. “Isothermal Oxidation Tests.” Scientific Notebook 617. San Antonio, Texas: CNWRA. pp. 41–69. 2004.

1 INTRODUCTION

Alloy 22 (Ni–22Cr–13Mo–4Fe–3W) was considered as the nuclear waste container material for the proposed Yucca Mountain repository (DOE, 2002). Under an igneous disruptive event, the waste container material may be deformed or damaged by molten magma at elevated temperatures. Therefore, the U.S. Department of Energy (DOE) analyzed waste package/magma interaction in analysis and model reports supporting the proposed Yucca Mountain repository license application (Bechtel SAIC, Company, LLC, 2004a,b,c; 2003). In the igneous activity scenario, significant pressure differences between ascending magma and open drifts cause magma to flow into the drifts and fill them upon intersection; thus, waste containers could be engulfed in magma. The ability of a waste container to withstand the combined thermal, chemical, and mechanical effects of magma exposure is uncertain.

To better understand the interaction of molten magma and high temperature exposure of Alloy 22 to oxidizing gases at elevated temperatures, The Center for Nuclear Waste Regulatory Analyses developed methodology and techniques to evaluate magma–Alloy 22 interaction. The techniques include thermogravimetric analysis (TGA) for dry-air oxidation and crucible tests for magma–Alloy 22 interaction experiments. These techniques and test results are described in this knowledge management report.

2 DRY-AIR OXIDATION

The oxidation kinetics of Alloy 22 in dry air was evaluated using TGA (Chiang and Mintz, 2008). The TGA technique requires continuous weighing of a sample in a specific environment at a constant temperature. This technique is widely used to study oxidation and high temperature corrosion. A schematic diagram of an automatic recording microbalance is shown in Figure 2-1. A photograph of a TherMax 700 microbalance that has a 1,700 °C [3,092 °F] temperature capability is shown in Figure 2-2. The oxidation test specimen is freely suspended from a precision microbalance located outside the furnace chamber. The microbalance mechanism records weight change due to chemical reactions on the alloy sample surface in a controlled environment, along with specimen temperature and elapsed time.

The Alloy 22 material was procured from Haynes International, Inc. (Kokomo, Indiana). The oxidation test specimens were machined from mill-annealed, 12.7-mm [0.5-in]-thick plate stock. The chemical composition of the material used in this study is provided in Table 2-1. The machined plate was cut into oxidation coupons sized 15 × 13 × 1.5 mm [0.6 × 0.5 × 0.06 in]. Specimens were wet surface ground to 600-grit silicon carbide paper and ultrasonically cleaned in an acetone bath and alcohol bath before oxidation exposure.

The oxidation rate data for Alloy 22 specimens subjected to isothermal oxidation in air at 850 and 1,100 °C [1,562 and 2,012 °F] are presented in Figure 2-3 as mass change versus square root of time. The oxidation mass change at a given exposure time is greater at 1,100 °C [2,012 °F] as compared to its counterpart at 850 °C [1,562 °F]. The results are as expected because the oxidation rate increases with increasing temperature. At both temperatures, the alloy exhibited a more rapid oxidation rate during an initial transient period of approximately 1.5 hours and a slower rate at longer times. For the 850 °C [1,562 °F] specimen, the data fall almost entirely along a straight line, indicating the oxidation kinetics obey a parabolic rate law that can be described in Eq (2-1):

$$m/A = (K_p t)^{1/2} + C \tag{2-1}$$

where m/A is the mass gain per unit area, K_p is the parabolic rate constant, and C is a constant. The mass gain during oxidation is the result of the mass of oxygen taken up in the oxide and in solution in the alloy. Wagner developed the theory of high temperature oxidation of metals under idealized conditions (Birks, et al., 2006). The theory describes the oxidation behavior for the case where the diffusion of ions in the metal is rate limiting and the oxidation rate follows a parabolic rate law. At the beginning of the high-temperature oxidation process at 850 °C [1,562 °F], oxidation proceeded at a rapid rate (Figure 2-3). After an initial transient oxidation period of approximately 1.5 hrs, a continuous chromia (Cr_2O_3) scale formed that acted as a barrier for outward diffusion of metallic elements and inward diffusion of oxygen. The oxidation rate after the transient oxidation period followed a parabolic rate law reasonably well, indicating the oxidization kinetics are controlled by outward diffusion of chromium through the Cr_2O_3 to form new oxide at the scale/gas interface. The parabolic rate constant (the square of the slope from Figure 2-3) for Alloy 22 at 850 °C [1,562 °F] is 5.1×10^{-4} mg^2/cm^{4}h [2.0×10^{-10} lb^2/in^{4}h]. At the higher temperature of 1,100 °C [2,012 °F], however, the data for the mass gain versus square root of time plot do not fit into a single straight line. The slopes of the plot keep decreasing with increasing exposure time, indicating the oxide growth mechanism may involve thinning of the oxide scale by vapor loss at the oxide/gas interface, causing divergence from a parabolic growth law.

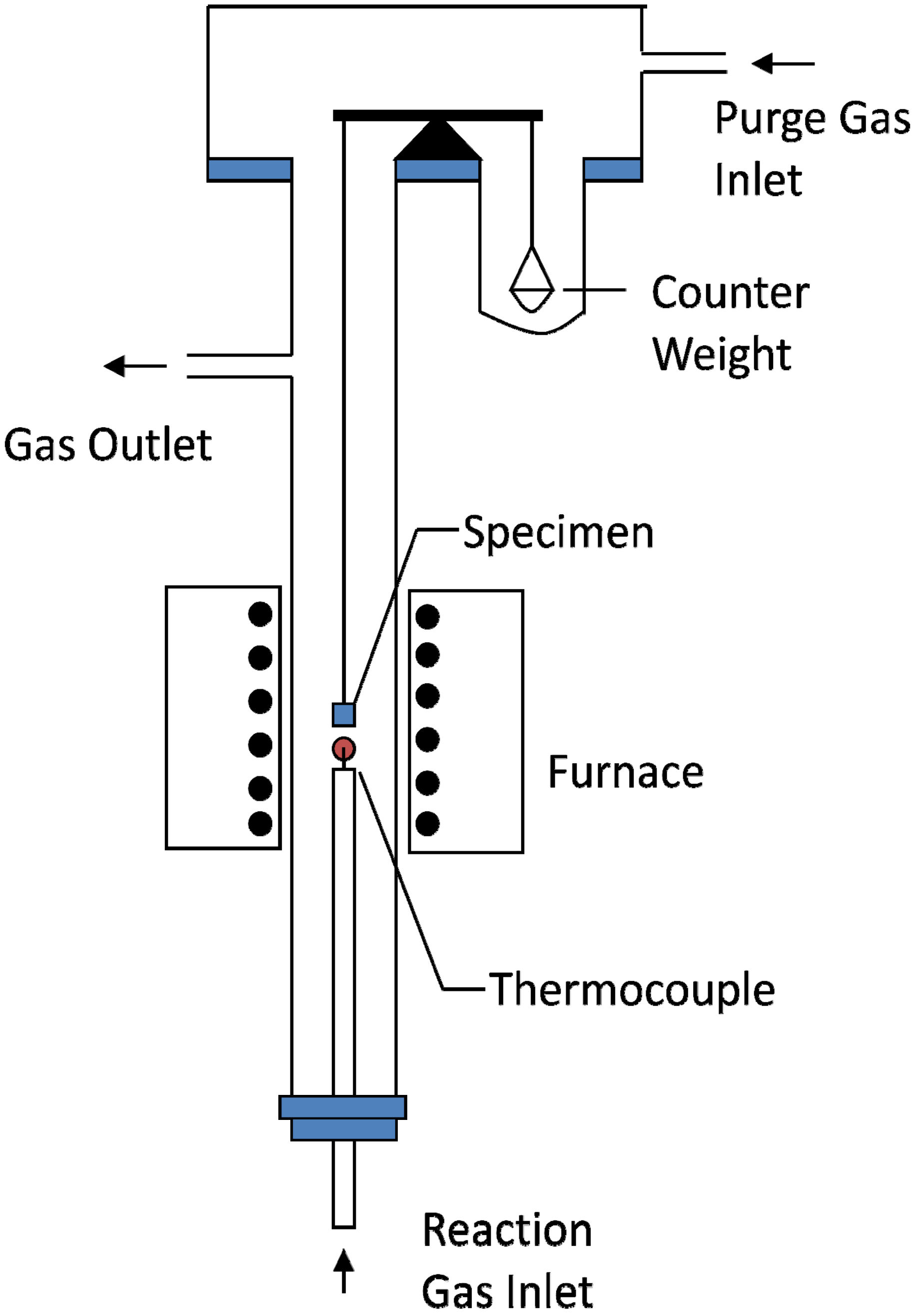

Figure 2-1. Schematic Diagram of a Thermogravimetric Apparatus With Automatic Recording Microbalance (Chiang and Mintz, 2008)

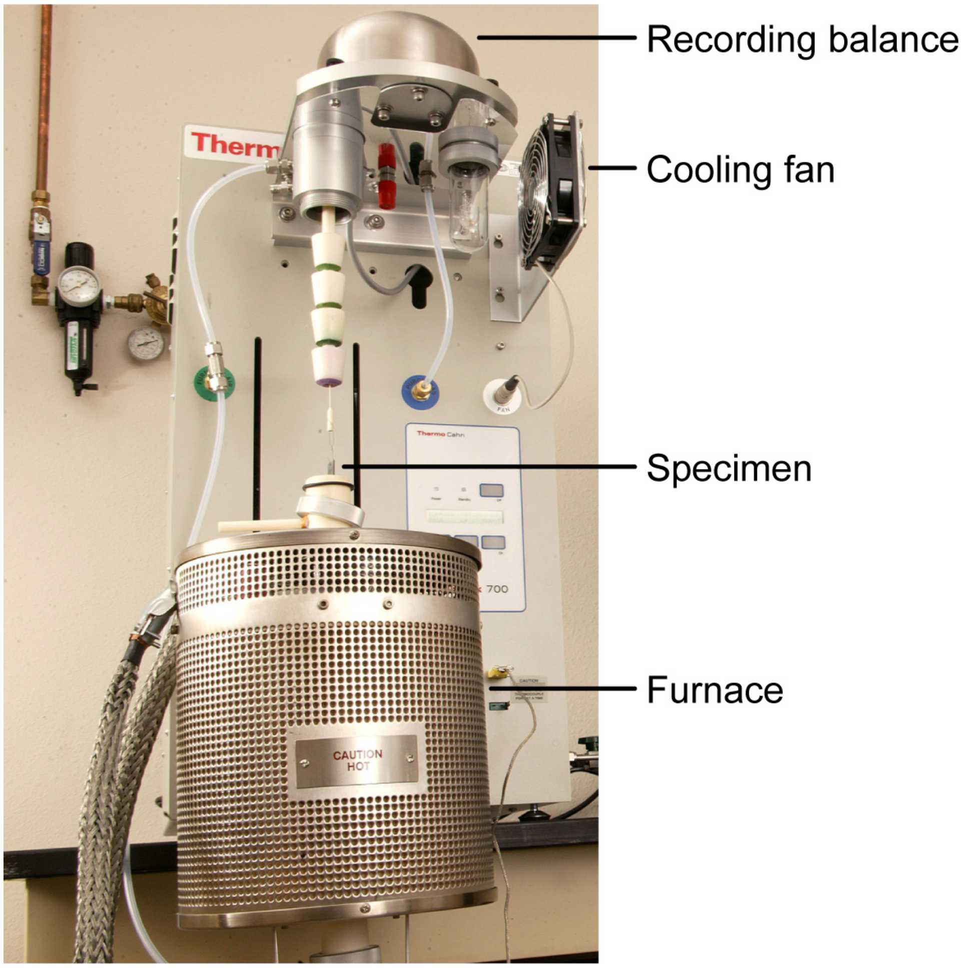

Figure 2-2. Photograph of a TherMax 700 Automatic Recording Microbalance at Southwest Research Institute®

Table 2-1. Chemical Composition (wt%) of Alloy 22 Plate

Material	Ni	Cr	Mo	W	Fe	Co	Si	Mn	V	P	S	C
Heat 2277-3-3266 12.7-mm [0.5-in]	Bal	21.40	13.30	2.81	3.75	1.19	0.03	0.23	0.14	0.008	0.004	0.005

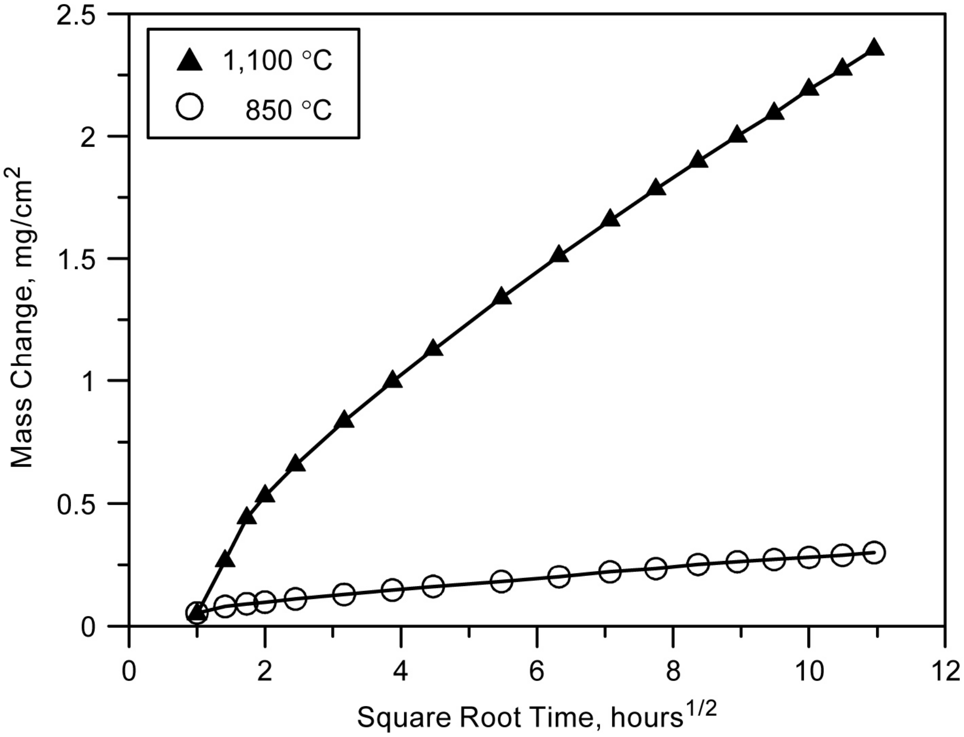

Figure 2-3. Dry-Air Oxidation Kinetics of Alloy 22 at 850 and 1,100 °C [1,562 and 2,012 °F] Plotted as Mass Change Versus Square Root of Time

After oxidation, cross sections of the test specimens were examined optically and with an electron microprobe and associated wavelength x-ray spectrometers. A backscattered electron image was taken of the surface oxide layer and the internal oxygen penetration region. Quantitative line scans of oxygen, chromium, iron, nickel, molybdenum, and tungsten were then run, starting at the surface and penetrating at 2-µm [79-µin] increments into the base material. A cross section view of the oxides that formed after exposure for 120 hours at 850 °C [1,562 °F] is shown in Figure 2-4(a). The elemental line scans of oxygen, chromium, iron, nickel, molybdenum, and tungsten are presented in Figure 2-4(b). The external scale consisted primarily of chromium and oxygen, indicating the oxide is Cr_2O_3. The Cr_2O_3 layer is approximately 4 µm [1.6×10^2 µin] thick. In several localized areas, internal oxide precipitates were also observed underneath the external scale. These internal oxides appeared as dark spots along grain boundaries in the backscattered electron micrograph in Figure 2-4(a). The maximum depth of inward oxygen penetration is approximately 4 µm [1.6×10^2 µin]. The composition profiles also show that there is a chromium depletion zone of about 8 µm [3.1×10^2 µin] underneath the external scale. No significant diffusion of iron, molybdenum or tungsten was observed. Similar trends were obtained at a higher temperature of 1,100 °C [2,012 °F] for the two oxidation periods of 24 and 120 hours. The thickness of the scale ranged from 2–4 µm [79–1.6×10^2 µin] in 24 hours and was 14 µm [551.2 µin] in 120 hours. Dissolution of oxygen into the alloy may also result in sub-surface precipitation of oxides of alloying elements (internal oxidation). Internal oxidation precipitates were observed deep into the alloy

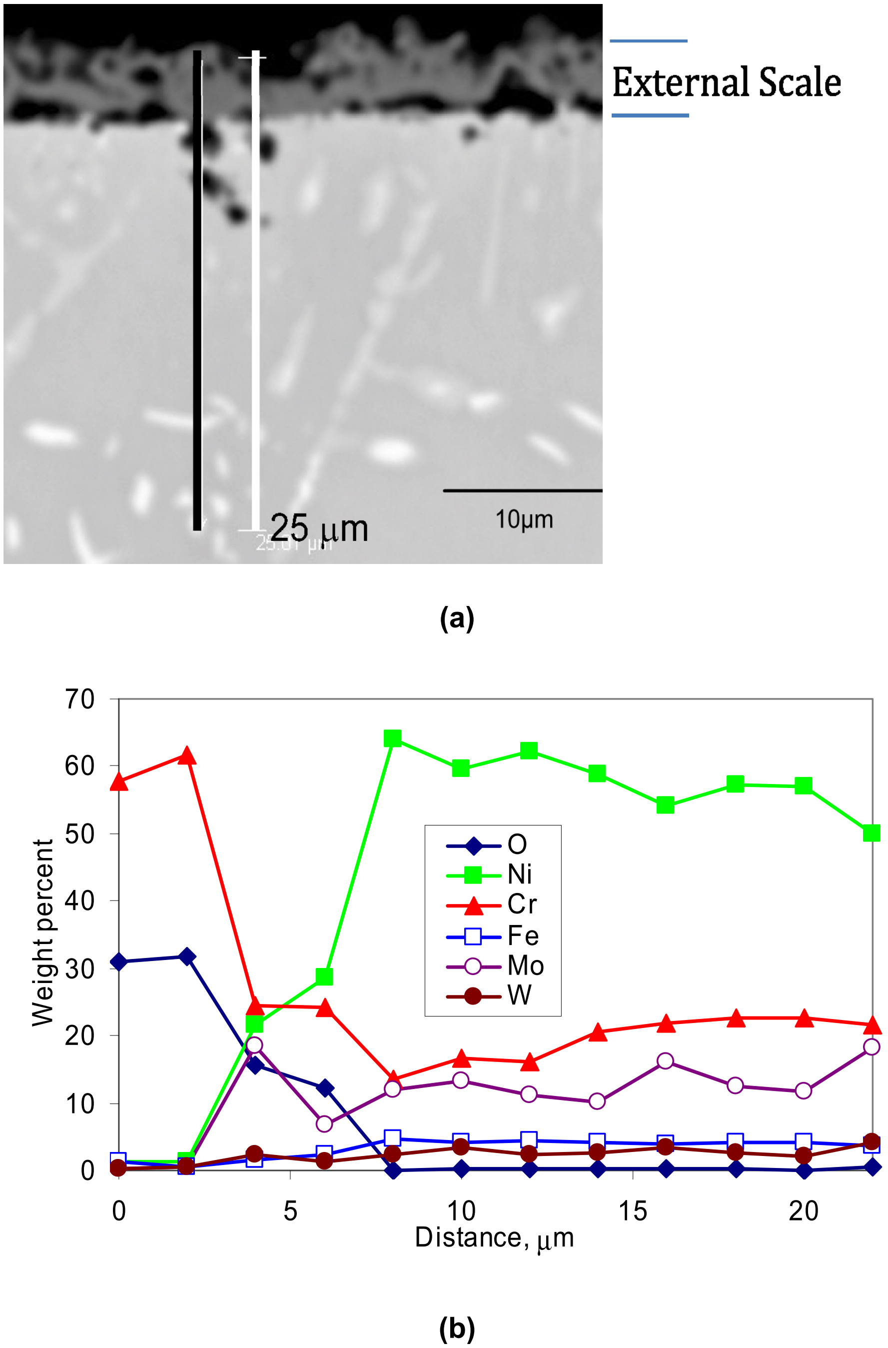

Figure 2-4. Cross Section Through the Scale Produced on Alloy 22 After 120 Hours Oxidation at 850 °C [1,562 °F]: (a) Scanning Electron Microscope Backscattered Electron Image and (b) Concentration Profiles of Oxygen, Chromium, Iron, Nickel, Molybdenum, and Tungsten Along the Line of Traverse Indicated in Figure 2-4 (a). The Oxide/Alloy Interface Is Located at Approximately 4-µm [3.9×10^2 µ in] Distance.

from 10 μm [3.9×10^2 μin] at 24 hours to 24 μm [9.5×10^2 μin] at 120 hours. The corrosion rate in terms of oxidation penetration depth was 5 to 10 μm/day [2.0×10^2 to 3.9×10^2 μin/day] at 850 °C [1,562 °F], which is consistent with formation of a continuous Cr_2O_3 scale for Ni-Cr alloys (see Figure 4-1).

3 MAGMA–ALLOY 22 INTERACTION

3.1 Analyses of Magma Samples from Lathrop Wells Volcano

To better understand the potential effects of magma contacting the Alloy 22 waste package container, samples of basalt were collected from lava flows produced by the Lathrop Wells volcano near Yucca Mountain. A set of 2.5-cm [1.0-in]-diameter core samples was collected from a location near the Lathrop Wells volcano and is identified as LW-4. To obtain the samples, a gasoline-powered, water-cooled coring device drilled the cores to a depth of 10 to 15 cm [4 to 6 in] into the surface of the Lathrop Wells lava flow. Representative core samples are shown in Figure 3-1(a).

The major chemical elements of the samples were analyzed using the energy dispersive x-ray analysis associated with the scanning electron microscope. Figure 3-1(b) shows the energy dispersive x-ray spectra of sample LW-4. The Lathrop Wells basalts contain silicon, aluminum, and iron oxides as major constituents. Minor amounts of calcium, magnesium, sodium, and potassium oxides are also present. DOE reported that the mean values listed as the major-element composition of Lathrop Wells basalts are (in oxide weight percent) SiO_2 (48.50), TiO_2 (1.93), Al_2O_3 (16.74), Fe_2O_3 (11.63), MgO (5.83), CaO (8.60), Na_2O (3.53), K_2O (1.84), and P_2O_5 (1.22) (Bechtel SAIC Company, LLC, 2004c, 2003). Therefore, the major and minor elements of the LW-4 basalt sample are consistent with those reported to be present in the literature. The LW-4 sample also contains manganese as a constituent element [Figure 3-1(b)]; however, the manganese distribution is a function of mineralogical phases, some of which are manganese-rich and others are manganese-poor.

The melting point of the basalt LW-4 sample was determined by heating a fragment of each sample in an alumina crucible above 1,100 °C [2,012 °F] in 20 °C [36 °F] increments until the basalt became molten. The Lathrop Wells sample LW-4 was molten at 1,150 °C [2,102 °F]. This temperature is a typical melting temperature for this type of basalt lava, obtained in other petrologic studies (Nicholis and Rutherford, 2004). This temperature was therefore selected for subsequent magma–Alloy 22 interaction experiments.

The high temperature corrosion experiment was performed by remelting Lathrop Wells basalts in crucibles of Alloy 22 to determine the alloy corrosion rate and oxidation behavior. The Alloy 22 crucibles were machined from mill-annealed, 25.4-mm [1-in]-diameter, 305-mm [12-in] bar stock. The bar material was confirmed to meet the chemical composition specified in ASTM B-575 for UNS N06022 alloy designation (ASTM International, 2004). The Alloy 22 bar stock was cut into 38.1-mm [1.5-in] sections and subsequently machined into a crucible. A drawing of an Alloy 22 crucible is presented in Figure 3-2. The 25.4-mm [1.0-in]-diameter by 38.1-mm [1.5-in]-long crucible was machined so that it had a cavity 19.1 mm [0.75 in] in diameter by 5.4 mm [1.0 in] deep. The sidewall thickness of the crucible was 3.2 mm [0.125 in] all around. The Alloy 22 crucible served two purposes: it was a container for the remelted basalts and Alloy 22 sidewalls were samples for evaluation of corrosion rate and oxidation behavior as the result of interaction with the remelted basalts.

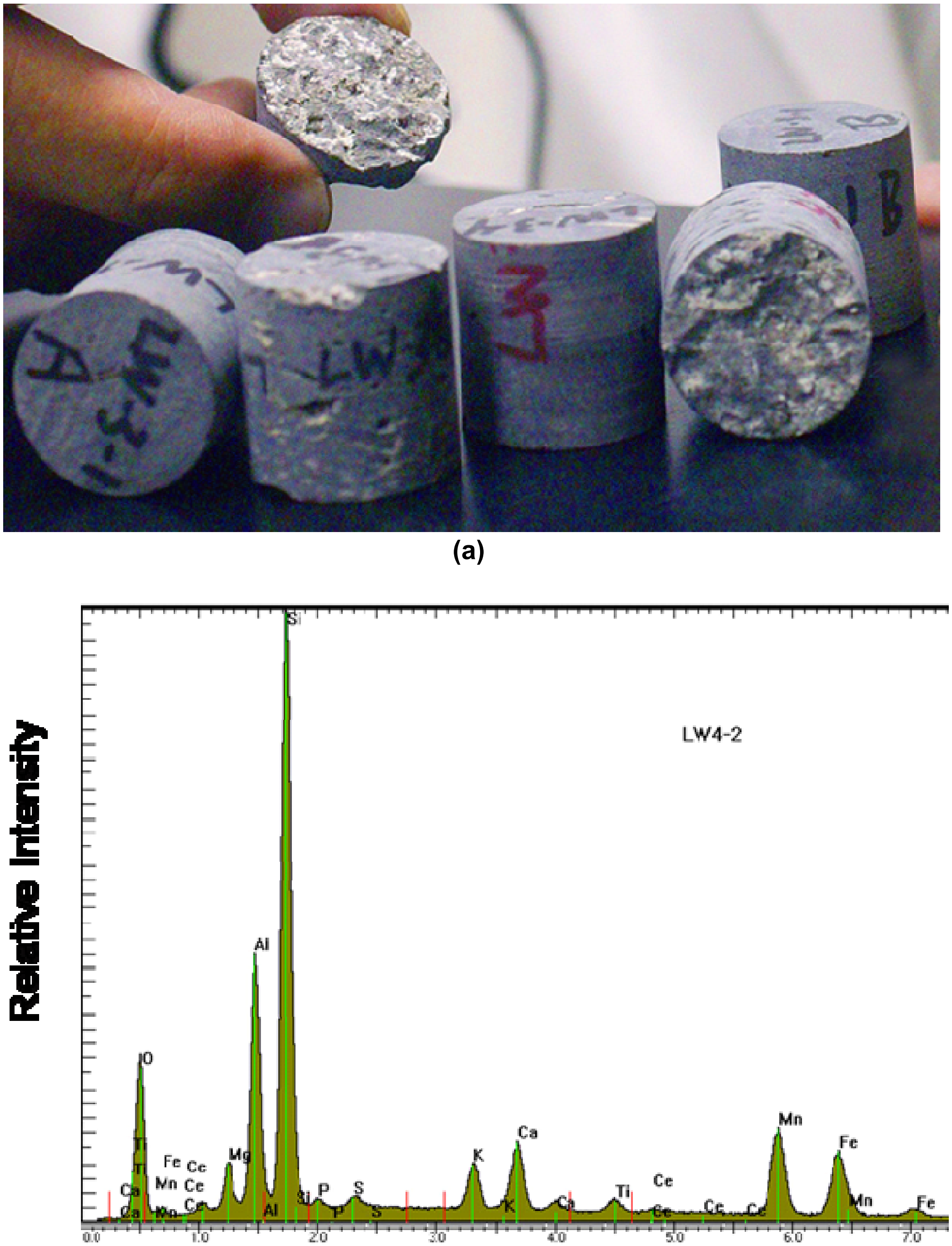

(a)

(b)

Figure 3-1. (a) Photograph of Magma Basalt Samples Collected From Lathrop Wells Volcano in Nevada and (b) Energy-Dispersive X-Ray Spectra of the Magma Sample

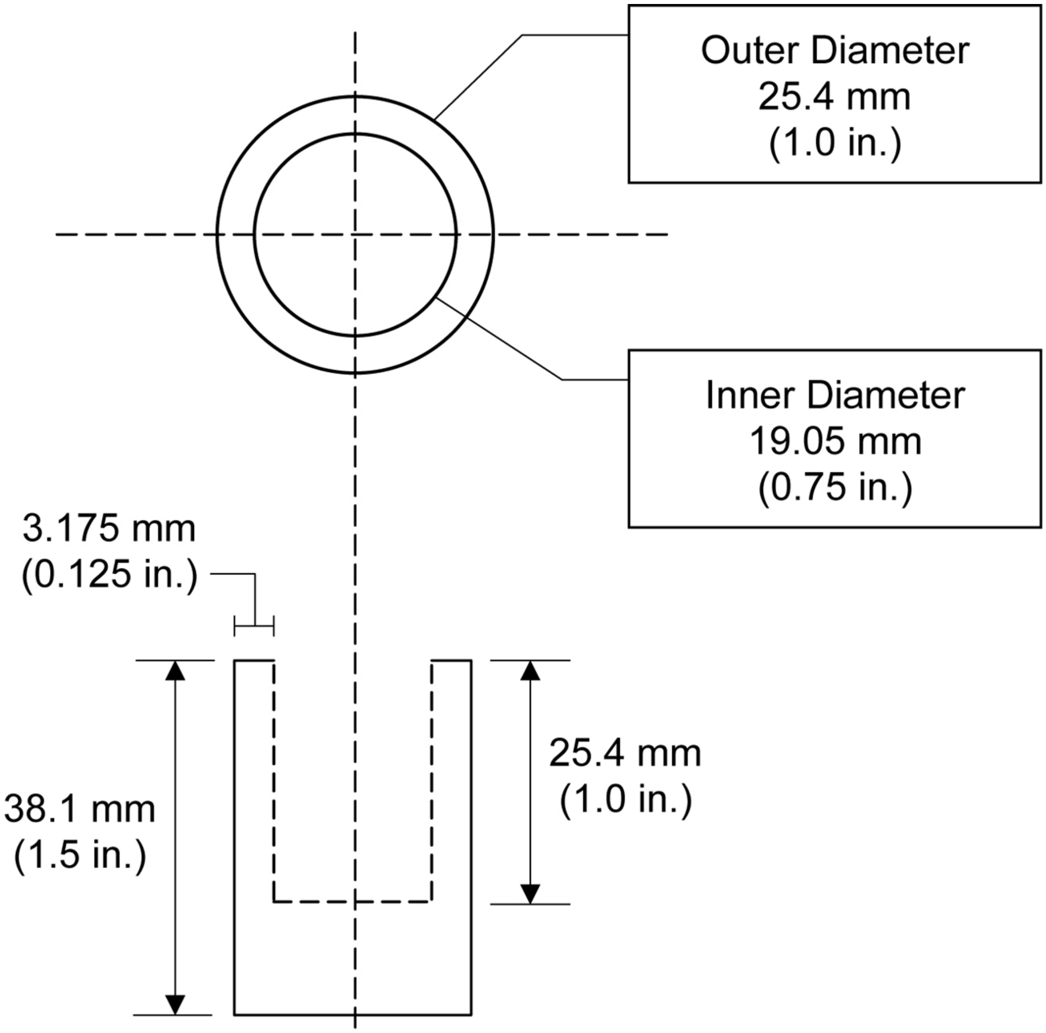

Figure 3-2. Drawing of the Alloy 22 Crucible for Magma–Alloy 22 Interaction Experiments

3.2 Alloy 22−Lathrop Wells Magma Interaction Experiments

To study the interaction between Alloy 22 and remelted Lathrop Wells basalt, an Alloy 22 crucible was filled with fragments of LW-4 basalt and heated in air to 1,150 °C [2,102 °F] for 65 hours. Figure 3-3(a,b) shows the appearance of samples before and after the magma–Alloy 22 interaction experiment. A large amount of non-protective oxides was formed on the inner wall of the crucible. These oxides were not adherent and spalled extensively during cooling to room temperature. X-ray diffraction analysis of the scales that were spalled off from the inner wall indicated that the oxides consisted of NiO and $NiCr_2O_4$ as major phases, and $Fe(Cr, Al)_2O_4$ and $NiMoO_4$ as minor phases. No chromia (Cr_2O_3) phase was identified. In Figure 3-3(c), the red lines denote the original Alloy 22 surfaces. The original Alloy 22 cylinder wall thickness was 3.125 mm [0.125 in]. The alloy wall thicknesses after the 65-hour (2.7 day) test were measured at 5 randomly selected locations with respect to the original alloy surface. The average of metal loss of 5 measurements was 677 μm [0.027 in] corresponding to a corrosion rate of 677 μm [0.027 in] days = 250 μm/day [0.01 μm/day]. The cross section of the top portion of the crucible [shown in Figure 3-3(c)] reveals that the molten Lathrop Wells basalt (henceforth called "magma"), had accelerated the corrosion rate of Alloy 22. The maximum alloy thickness loss occurred at Point A (Figure 3-3c). The measured metal thickness loss was 1,230 μm [0.048 in]. The corresponding maximum metal thickness loss rate was 1,230 μm [0.048 in]/2.7 days = 455 μm/day [17,900 μin/day].

Figure 3-4(a,b) presents scanning electron micrographs of cross sections of the specimen after the magma–Alloy 22 interaction experiment. The figure illustrates two types of oxidation behavior that were observed in magma–Alloy 22 interaction. Figure 3-4(a) shows that above the magma Alloy 22 interface, oxidation resulted in a high rate of metal loss by the formation of porous, nonprotective oxides. However, these porous oxides were spalled off and not shown in Figure 3-4(a). Vesicles and a nonuniform distribution of phases were observed in the magma. Beneath the interface where the metal solid, molten magma, and gaseous oxygen coexisted, however, the Alloy 22 in contact with the molten magma oxidized at a much slower rate. Figure 3-4(b) shows a higher magnification view of the magma–Alloy 22 interface away from the air interface. At these locations, the oxygen partial pressure was reduced and a continuous chromia scale is clearly delineated. The chromia scale thickness ranged from 12 to 23 μm [4.7×10^2 to 9.1×10^2 μin]. This oxidation behavior corresponds to a low corrosion rate of approximately 10 to 20 μm/day [3.9×10^2 to 7.9×10^2 μin/day]. Inside the Alloy 22, oxygen also diffused inward to form oxide precipitates, especially along grain boundaries. The depth of oxygen penetration inward was estimated to be 30 μm [1.2×10^3 μin].

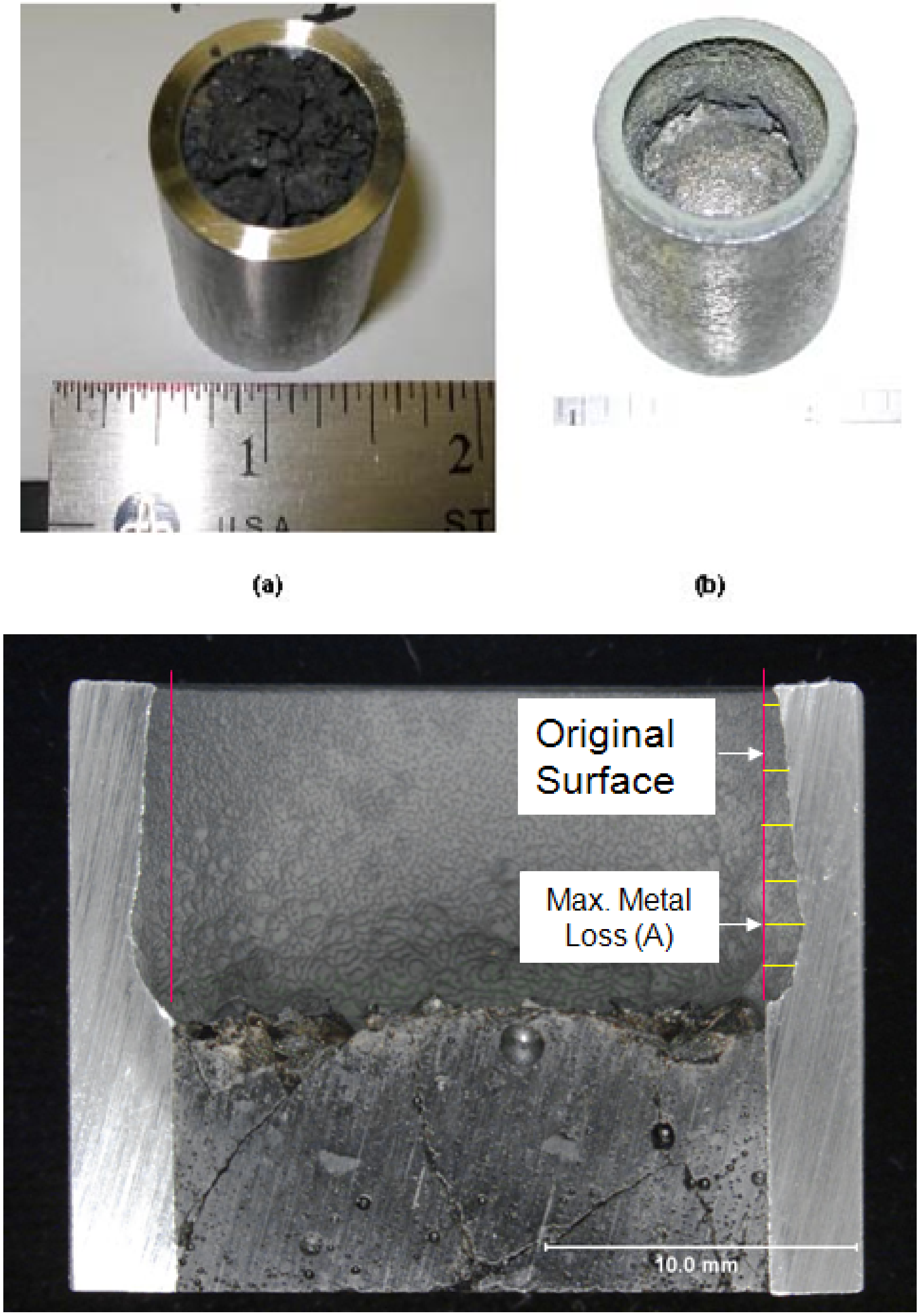

(a) (b)

(c)

Figure 3-3. Photograph of Alloy 22 Crucible With LW-4 Basalt. (a) Before Test; (b) After Exposure to 1,150 °C [2,102 °F] in Air for 65 Hours; and (c) Cross-Sectional View of (b) Top Portion. Note: Red lines denote original alloy surface, yellow lines show locations where metal thickness losses and maximum thickness loss (point A) were measured.

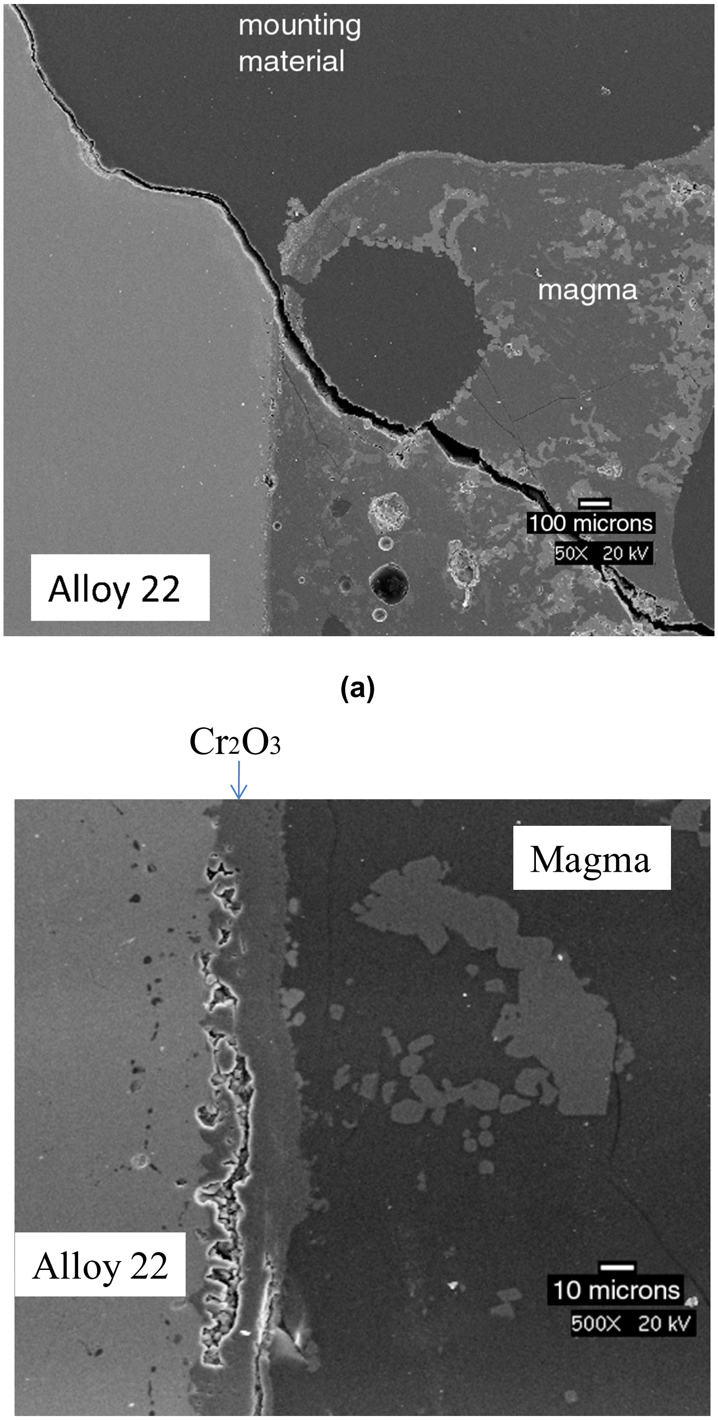

(a)

(b)

Figure 3-4. Scanning Electron Micrographs Showing Cross Sections of Alloy 22 Crucible After Interaction With LW-4 Samples for 65 Hours in Air: (a) at the Magma–Alloy 22–Air Interface, (b) at the Magma–Alloy 22 Interface Away From the Air Interface.

4 ANALYSIS OF RESULTS AND DISCUSSION

The commercially available structural materials for high-temperature components are based on the systems of Ni-Cr, Ni-Fe-Cr, or Fe-Cr due to the formation of protective Cr_2O_3 scale (Lai, 1990). The Alloy 22 contains high amounts (nominally 22 weight percent) of the oxide-forming element Cr, which by selective oxidation during high-temperature exposure forms slow-growing surface oxide scales of Cr_2O_3, protecting the material against rapid attack by oxidizing environments (Dunn, et al., 2005; Pensado, et al., 2006).

In the present study, accelerated oxidation of Alloy 22 by molten magma was observed at the interface where solid alloy, liquid magma, and gaseous phases coexisted. The gaseous phases included oxygen from air and magmatic gases released from the molten magma. The effectiveness of chromia scale at the interface can be reduced at elevated temperature in two ways. First, at a temperature above 1,100 °C [2,012 °F], thinning of Cr_2O_3 scale by vapor loss is significant at the oxide/gas interface. The gaseous species in equilibrium with Cr_2O_3 scale include Cr(g), CrO(g), CrO_2(g), and CrO_3(g) (Birks, et al., 2006). Second, the constituent phases in the molten magma, such as calcium oxide (CaO), can react with Cr_2O_3 to form oxides (e.g., $CaCrO_4$) that may prevent the formation of continuous, protective scale. Chiang, et al. (1984) studied the effect of CaO on oxidation behavior of Cr_2O_3-forming alloys in the temperature range of 850 to 1,050 °C [1,562 to 1,922 °F]. The study reported that CaO accelerates the degradation of Cr_2O_3-forming alloys in air or oxygen by two mechanisms: (i) acceleration of CrO_3 evaporation and (ii) liquid formation by reaction of CaO and Cr_2O_3 at temperatures above 1,000 °C [1,832 °F], which results in catastrophic corrosion. Further work would be needed to better understand the accelerated corrosion of Alloy 22 at the magma–Alloy 22 interface.

The oxidation and corrosion rates alloys are strongly dependent on partial pressure of oxygen in the high temperature environment (Birks, et al., 2006). In this study, two types of oxidation behavior were observed in two different oxygen partial pressure environments. At the lower portion of the crucible where the oxygen partial pressure is low, a low corrosion rate of 10 to 20 μm/day [3.9×10^2 to 7.9×10^2 μin/day] was observed. At the top portion of the crucible where the Alloy 22 surface was exposed in air (high oxygen partial pressure), a high corrosion rate of 250–455 μm/day [9.8×10^3–1.8×10^4 μin/day] was observed at the magma melting point of 1,150 °C [2,102 °F]. The two different oxidation rates are shown in Figure 4-1, and are compared with the oxidation rates for Ni-Cr alloys measured at lower temperatures (< 840 °C [1,544 °F]). It should be noted that the high corrosion rate was obtained under air, which may not simulate basaltic magma conditions. Electric Power Research Institute (2004) immersed Alloy 22 samples in molten magma at a temperature of 1,200 °C [2,192 °F] in an inert atmosphere to simulate a basaltic magma environment. A maximum penetration depth of approximately 200 μm [7.9×10^3 μin] was observed after one week. The depth corresponds to a corrosion rate of about 30 μm/day [1.2×10^3 μin/day]. The results are consistent with oxidation of Alloy 22 in low oxygen partial pressure forming a continuous Cr_2O_3 scale, as obtained in this study (Figure 3-4b).

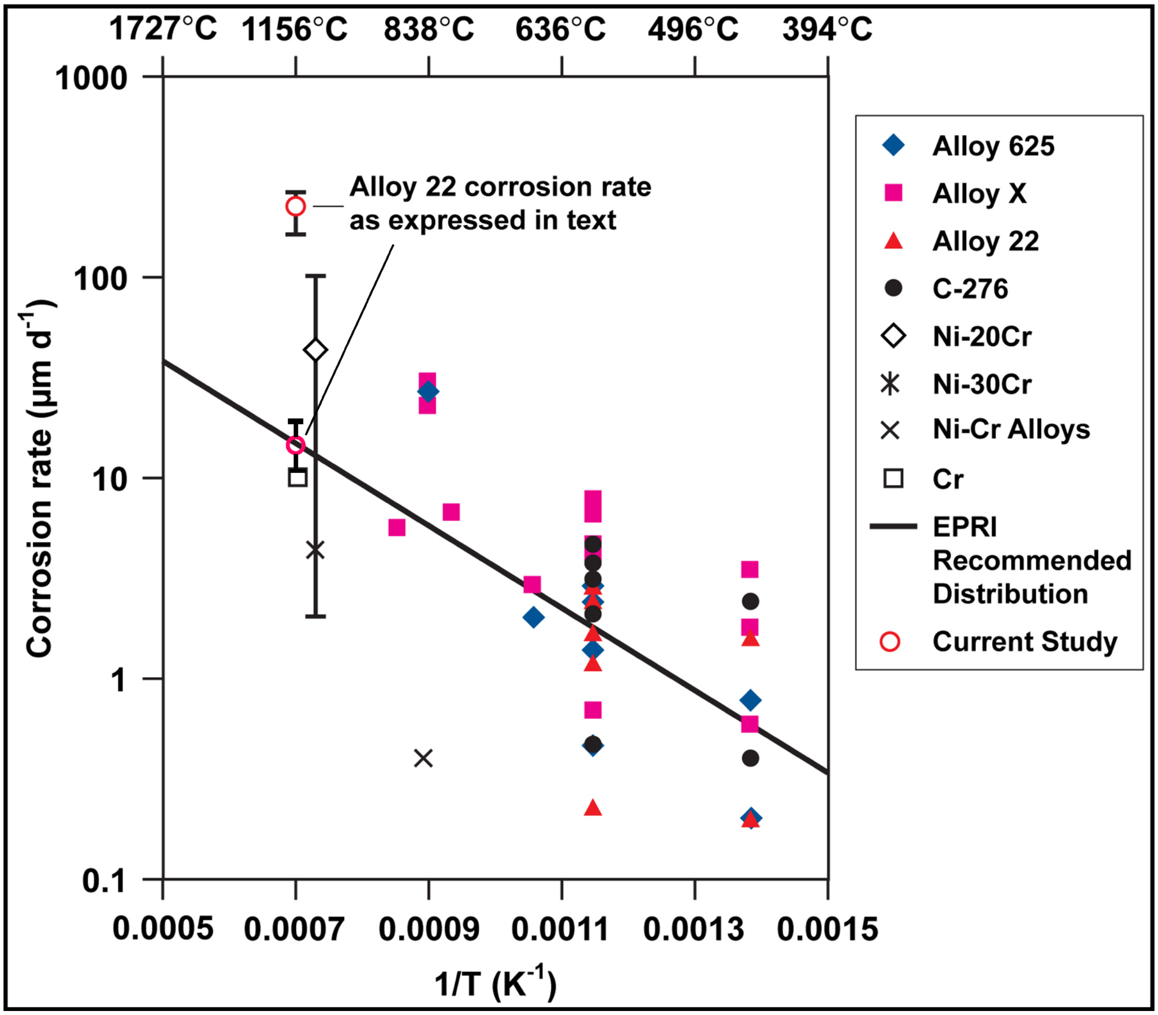

Figure 4-1. Comparison of High-Temperature Corrosion Rate of Alloy 22 in the Presence of Remelted Lathrop Wells Basalt at 1,150 °C [2,102 °F] in Air With Published Data on Ni-Cr Alloys. The Compilation of Corrosion Rate Data and Recommended Distribution Is Adapted From Electric Power Research Institute (2004).

5 SUMMARY AND CONCLUSIONS

An independent evaluation of magma–Alloy 22 interaction was conducted. Methodology and experimental techniques were developed to evaluate (i) dry-air oxidation of Alloy 22 using TGA techniques and (ii) interaction between magma and Alloy 22 by remelting Lathrop Wells basalt in crucibles of Alloy 22. The following conclusions can be drawn:

- TGA can produce oxidation kinetics data under controlled environment, temperature and time. At a temperature of 850 °C [1,562 °F], the oxidation kinetics of Alloy 22 follows a parabolic rate law indicating the oxide growth is diffusion controlled.

- The interaction of molten Lathrop Wells magma with Alloy 22 at 1,150 °C [2,102 °F] resulted in two types of oxidation morphology. Accelerated corrosion was observed at the interface where solid metal, liquid magma, and gaseous oxygen coexisted. The estimated corrosion rate ranged from 250 to 455 µm/day [9.8×10^3 to 1.8×10^4 µin/day]. It should be noted that the high corrosion rate of Alloy 22 was obtained under air, which may not be representative of the conditions of basaltic magmas. This rate is approximately one order of magnitude higher than the 10 µm/day [3.9×10^2 µin/day] corrosion rate characteristic of protective scale formation on the Alloy 22 surface in this temperature range. At locations with low oxygen partial pressure, the alloy formed continuous chromia scale at a low oxidation rate similar to that of dry-air oxidation.

6 REFERENCES

ASTM International. “Standard Specification for Low-Carbon Nickel-Molybdenum-Chromium, Low-Carbon Nickel-Chromium-Molybdenum, Low-Carbon Nickel-Chromium-Molybdenum-Copper, Low-Carbon Nickel-Chromium-Molybdenum-Tantalum, and Low-Carbon Nickel-Chromium-Molybdenum-Tungsten Alloy Plate, Sheet, and Strip.” ASTM B–75–04a. West Conshohocken, Pennsylvania: ASTM International. 2004.

Bechtel SAIC Company, LLC. “Igneous Intrusion Impacts on Waste Packages and Waste Forms.” MDL–EBS–GS–000002. Rev. 1. Las Vegas, Nevada: Bechtel SAIC Company, LLC. 2004a.

_____. “Characterize Eruptive Processes at Yucca Mountain, Nevada.” ANL–MGR–GS–000002. Rev. 02. Las Vegas, Nevada: Bechtel SAIC Company, LLC. 2004b.

_____. “Dike/Drift Interactions.” MDL–MGR–GS–000005. Rev. 1. Las Vegas, Nevada: Bechtel SAIC Company, LLC. 2004c.

_____. “Technical Basis Document No.13: Volcanic Events.” ANL–MGR–GS–000002. Rev. 02. Las Vegas, Nevada: Bechtel SAIC Company, LLC. 2003.

Birks, N., G.H. Meier, and F.S. Pettit. *Introduction to the High-Temperature Oxidation of Metals.* 2nd Edition. New York City, New York: Cambridge University Press. 2006.

Chiang, K.T. and T. Mintz. “Gravimetric Techniques. ” *Techniques for Corrosion Monitoring.* L. Yang, ed. Chapter 9. Cambridge, England: Woodhead Publishing Limited. pp. 247–264. 2008.

Chiang, K.T., G.H. Meier, and R.A. Perkins. “The Effect of Deposits of CaO, $CaSO_4$, and MgO on the Oxidation of Several Cr_2O_3-Forming and Al_2O_3-Forming Alloys.” *Journal of Materials for Energy Systems*. Vol. 6, No. 2. pp. 71–86. 1984.

DOE. DOE/RW–539–1, “Yucca Mountain Science and Engineering Report.” Las Vegas, Nevada: DOE, Office of Civilian Radioactive Waste Management. February 2002.

Dunn, D.S., O. Pensado, Y.-M. Pan, R.T. Pabalan, L. Yang, X. He, and K.T. Chiang. “Passive and Localized Corrosion of Alloy 22–Modeling and Experiments.” CNWRA Report 2005-02. San Antonio, Texas: CNWRA. 2005.

Electric Power Research Institute. “Potential Igneous Processes Relevant to the Yucca Mountain Repository: Extrusive-Release Scenario Analysis and Implications.” EPRI TR–1008169. Palo Alto, California: Electric Power Research Institute. 2004.

Lai, G.Y. “High-Temperature Corrosion of Engineering Alloys.” Materials Park, Ohio: ASM International. 1990.

Nicholis, M.G. and M.J. Rutherford. “Experimental Constraints on Magma Ascent Rate for the Crater Flat Volcanic Zone Hawaiite.” *Geology*. Vol. 32, No. 6. pp. 489–492. 2004.

Pensado, O., R. Pabalan, D. Dunn, and K.T. Chiang. "Use of Alloy-22 as a Long-Term Radioactive Waste Containment Material." Passivation of Metals and Semiconductors, and Properties of Thin Oxide Layers—A Selection of Papers from the 9th International Symposium. Paris, France, June 27–July 1, 2005. Phillipe Marcus and Vincent Maurice, eds. The Netherlands: Elsevier. pp. 53–57. 2006.